HOSTED BY
ELSEVIER
Available online at www.sciencedirect.com
ScienceDirect
Soils and Foundations xxx (2017) xxx–xxx
SOILS AND FOUNDATIONS
www.elsevier.com/locate/sandf

Determination of the critical state of granular materials with triaxial tests

E. Salvatore [a], G. Modoni [a,*], E. Andò [b,c], M. Albano [a,d], G. Viggiani [c,b]

[a] University of Cassino and Southern Lazio, Italy
[b] CNRS, 3SR, F-38000 Grenoble, France
[c] Université Grenoble Alpes, 3SR, F-38000 Grenoble, France
[d] INGV – National Institute of Geophysics and Vulcanology, Italy

Received 12 June 2016; received in revised form 18 May 2017; accepted 28 May 2017

Abstract

While the Critical State Locus (CSL) determined from triaxial compression tests is commonly adopted for the constitutive modelling of soil, the validity of the locus for other stress paths needs to be proved. Several authors have tried to experimentally verify whether the classical CSL representation in the stress invariants – void ratio space could be considered as unique or should depend on the loading direction, but the question is still being debated and a unique conclusion has not been convincingly drawn. In order to clarify this issue, compression and extension triaxial tests are performed on granular materials with different characteristics, namely, two homogeneously distributed sands and an assembly of steel spheres prepared under different initial conditions. The procedure for identifying the CSL is reviewed and indicates the limitations arising from strain localization (shear bands and necking). All the tests show that the materials head to systematically different traces in the e-p' and p'-q planes when sheared under triaxial compression and extension. Searching for the reasons for this phenomenon, small samples of sand are subjected to the same tests quantifying the whole strain field with X-ray tomography and a digital image correlation. This analysis reveals an inhomogeneous pattern of deformation that is strongly affected by the presence of the two rigid frictional bases and the flexible side membrane, even for the samples deforming in an apparently uniform manner. The different localization observed for the compression and extension tests justifies the dependence of the CSL on the stress path seen on the global scale. On the other hand, a unique trace of the CSL is obtained in the volumetric e-p' plane when the void ratio is measured limitedly to the zones affected by the largest distortion.

Keywords: Critical state; Granular soil; Triaxial tests; Stress path; Anisotropy; Strain localization

1. Introduction

In the conventional schematic representation of the mechanical soil response with stresses, strains and state variables, an analogy is implicitly assumed between the particulate materials and the continuum. It stems from this assumption that constitutive relations are inferred from laboratory tests with a macroscopic phenomenological approach, computing forces and displacements at the sample boundaries and that they are considered to be uniformly distributed over the whole volume. In this way, the particulate nature of the material is forgotten, despite the fact that the macroscopically observed response is often a summary of the complex patterns of local discontinuities (Lam and Tatsuoka, 1988).

Such a discrepancy becomes more relevant and implications need to be taken into account when the soil is sheared up to its ultimate condition. The importance of this state

Peer review under responsibility of The Japanese Geotechnical Society.
* Corresponding author.
E-mail address: modoni@unicas.it (G. Modoni).

https://doi.org/10.1016/j.sandf.2017.08.005
0038-0806/

on the soil deformation has been progressively acknowledged and is presently a footstone of soil mechanics. Casagrande (1936) firstly observed that granular materials, initially compacted at different densities, tend to contract or dilate and eventually reach a unique condition when sheared with the same normal stress. In this state, termed *critical*, the volume and shear stress remain steadily constant along with the distortion of the sample. Subsequently, Wroth (1958) found that the final void ratio and shear stresses are related to the applied normal effective stress and are independent of the previously given stress history. In both cases, the authors refer to a simple shear mechanism, where normal and shear stresses acting on the failure plane are given, while the stress components out of this plane are unknown.

Thereafter, the Critical State concept was extended to triaxial compression (*e.g.*, Roscoe et al., 1958; Poorooshasb, 1961; Thurairajah, 1961; Vesic and Clough, 1968) using tests where the stress components acting on each plane were completely known. In an attempt to generalize the definition of the Critical State, normal and shear stresses were then replaced by mean effective and deviator stress invariants, respectively. Now the Critical State Locus (henceforth referred to as CSL) commonly designates the curve in the p'-q-e space defined by the following expressions (Schofield and Wroth, 1968):

$$\begin{aligned} e &= \Gamma - \lambda \cdot \ln p' \\ q &= M \cdot p' \end{aligned} \tag{1}$$

The CSL has increasingly become a fundamental concept for interpreting the mechanics of granular materials, having been validated by plenty of experimental campaigns. In particular, it has been adopted in a class of popular constitutive models as a reference for justifying the combined dependency of the soil response on the present void ratio and stresses (*e.g.*, Jefferies, 1993; Muir Wood et al., 1994; Manzari and Dafalias, 1997; Modoni et al., 2011) or for evaluating the seismic liquefaction potential of saturated loose sands based on their static behaviour (Poulos et al., 1985; Jafarian et al., 2013).

Indeed, due basically to experimental difficulties, the CSL is inferred, with few exceptions, from the results of drained or undrained triaxial compression tests ($\sigma'_1 > \sigma'_2 = \sigma'_3$) (*e.g.*, Verdugo and Ishihara, 1996; Flora et al., 2012). A generalisation of the models to other stress conditions, such as triaxial extension, cyclically alternated compression and extension or, more generally, to multiaxial stress states, is rarely provided (*e.g.*, Chiaro et al., 2013) or is sometimes accomplished by implicitly assuming that the parameters of Eq. (1) (Γ,λ) are independent of the loading direction (*e.g.*, Manzari and Dafalias, 1997; Gajo and Muir Wood, 1999; Reza Imam et al., 2005). The use of mean effective stress and deviator stress p' and q in Eq. (1) may give the impression that the CSL can be uniquely defined, irrespective of the adopted stress path (*i.e.*, the relative magnitude between all the stress components). Indeed, the stress tensor in a point is completely defined by six independent variables. Therefore, the independence of the Critical State parameters, from all the variables other than p' and q, is just a simplification and cannot be postulated without experimental validation or a theoretical demonstration.

A key assumption for the uniqueness of the CSL is that the initial soil fabric and a memory of the loading history are erased by the large deformations experienced to reach the Critical State. The non-directional soil texture in this final condition is uniquely expressed in Eq. (1) by void ratio e, which represents a cumulative index of the soil state not taking into account the possible directional dependency of the void spaces and the distribution. Thus, the soil response is governed by the friction developing in a fully remoulded material. Such a postulate does not seem to have generally gained agreement in the literature. In fact, while experiments conducted by Been et al. (1991) exhibit a unique Critical State line in the e-p' plane for undrained compression and extension tests, *i.e.*, for two loading conditions causing opposite distortional effects, different pieces of evidence emerge from the work of other authors. Among them, Vaid and Chern (1985) observe that the response of a sand subjected to undrained triaxial extension ($\sigma'_1 = \sigma'_2 > \sigma'_3$) is by far more contractive than during compression. Subsequent studies showed similar friction angles, but different traces of the CSL in the e-p' plane for compression and extension tests (Vaid et al., 1990; Vaid and Thomas, 1995; Riemer and Seed, 1997). More particularly, extension tests tend to reach lower final void ratios than compression tests at the same p' value. Furthermore, a dependency of the Critical State Line obtained with extension tests on the sample preparation technique and on the initial effective confining stress was observed. All this evidence seems to imply that the depositional history of the soil fabric is not totally erased by shearing, but that some memory still persists even at the critical state (Fonseca et al., 2013). These observations form the basis for the definition of a critical state theory including the role of inherent anisotropy (Li and Dafalias, 2002; Dafalias and Manzari 2004; Dafalias et al., 2004; Papadimitriou et al., 2005), subsequently modified by Li and Dafalias (2012) with an evolving fabric tensor.

In support of the stress path dependency of the CSL are the observations of Riemer and Seed (1997) and Yoshimine et al. (1998), both exhibiting lower Critical State traces of the e-p' plane lines in extension tests than for those in compression tests. However, there is a discrepancy between these two studies and it is related to the position of the Critical State Line obtained from simple shearing. In fact, while ultimate steady state void ratios from undrained hollow cylinder torsional shear tests (Yoshimine et al., 1998) fall within the values found for undrained triaxial compression and extension tests at the same p', Riemer and Seed (1997) found absolute lower void ratios in simple shear tests compared with the other shear modes. For the sake of clarity, it must be argued that an evaluation of the normal stress components in simple shear tests, which

Please cite this article in press as: Salvatore, E. et al., Determination of the critical state of granular materials with triaxial tests, Soils Found. (2017), https://doi.org/10.1016/j.sandf.2017.08.005

represents a necessary step in calculating p', is very delicate and not free from uncertainties.

Finally, a more recent experimental study, involving partially drained tests performed under constant shear stress (Yoshimine and Kataoka, 2007) gave insignificant differences between triaxial compression and extension steady state lines in the e-p' plane. A more careful analysis of these data and of the previously recalled work of Been et al. (1991) highlights that the CSL is evaluated in both cases at particularly low values for p' (between 10 and 100 kPa), while tests in other studies are conducted at larger mean effective stresses. This comparison suggests that the role of the stress level on the uniqueness of the CSL may be significant.

A possible explanation for the stress path dependency of the Critical State is provided by Li and Dafalias (2002) in light of the inherent fabric anisotropy of the soil deposited in the gravitational field. In their analysis, based on the micromechanical observations of Oda and Nakayama (1988), the authors attribute the anisotropy of the soil behaviour to the preferential orientation of the particle contacts, void spaces and non-spherical particles, claiming the latter as the only factor surviving the large deformations necessary to reach the Critical State. Based on this assumption, the authors formulate a directional definition of the CSL through a scalar-valued variable accounting for the deviation between the principal stresses and the orientation of the particles. This model is advantageous in that it places the attention on the particulate granular nature of cohesionless materials, searching for a link between the macroscopic laboratory observations and the simple microscopic mechanisms. However, the model implicitly assumes that the stress path dependency of the CSL is a prerogative of the anisotropic shaped grains, since a unique CSL is obtained for the isotropic particles independently of the stress tensor applied at the Critical State.

The scope of the present paper is to experimentally investigate the role of the stress path on the CSL position clarifying the nature of the deformation in triaxial tests. With this aim in mind, a classical phenomenological analysis, based on conventional laboratory tests, is combined with the observation of the spatial distributions of the voids within the sample obtained from X-ray microtomography. The experimental study, confined to triaxial compression and extension tests, has been conducted on three different materials, two natural sandy soils with different grain size compositions as well as an assembly of uniform steel spheres. The latter represents an ideal, perfectly isotropic material because, even considering an initial orientation of the contacts and voids given by the gravity deposition, they are erased by the high isotropic stresses applied during the tests.

2. Conventional laboratory tests

This experimental program consists of a series of triaxial tests performed at a controlled strain rate ($\dot{\varepsilon}_a \approx 5\%/\text{hr}$) on cylindrical specimens having a diameter and a height of 70 and 140 mm, respectively. All samples were formed at various densities (dry pluviation and tamping were adopted to create loose and dense samples, respectively) and then carefully saturated (Skempton B values ranged from 0.94 to 0.98). Shearing was performed up to distortional strains always larger than 25% starting from various initial mean effective stresses (from 50 to 700 kPa) and following different stress paths (constant confining or mean effective stresses).

The tested materials consist of two uniformly graded sandy soils (Fossanova S3 and Hostun H31) and an assembly of steel spheres having the grain size distributions depicted in Fig. 1. The Fossanova sand presents subangular to subrounded grains made of quartzitic mica (Fig. 2a), while the Hostun sand is made of angular siliceous particles (Fig. 2b). Assemblies of steel spheres, having a diameter equal to 3 mm and controlled with a precision of 10 μm, were also tested. They represent an example of inherently isotropic material. The complete list of tests performed on the Fossanova sand and the steel spheres is reported in Table 1.

The term Critical State is used to describe a condition whereby the soil undergoes indefinite distortion without changing the volume or effective stresses. However, since this condition is typically attained at large strains, shear bands localized in relatively narrow regions often appear in advance (*e.g.*, Mooney et al., 1998) and make the strain distribution of the sample largely inhomogeneous (*e.g.*, Riemer and Seed, 1997). This phenomenon prevents the homogeneous distribution of volumetric strains in the sample, making their measurement with conventional techniques (*e.g.*, water expelled/adsorbed from the sample) no longer representative. In the tests performed on Fossanova sand (Modoni and Gazzellone, 2011), shear banding occurred on dense samples subjected to low initial mean effective stresses, *i.e.*, on samples requiring large volume changes to reach the CSL, but was not visible on relatively loose samples that deformed with the classical barrel shape. With these tests, the CSL trace in the e-p' plane could also

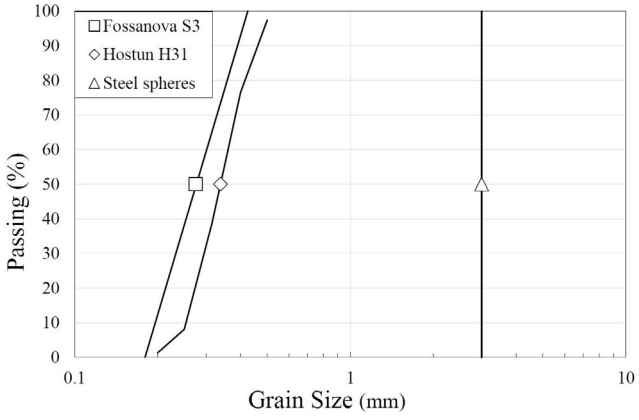

Fig. 1. Grain size distributions of the three tested materials.

Please cite this article in press as: Salvatore, E. et al., Determination of the critical state of granular materials with triaxial tests, Soils Found. (2017), https://doi.org/10.1016/j.sandf.2017.08.005

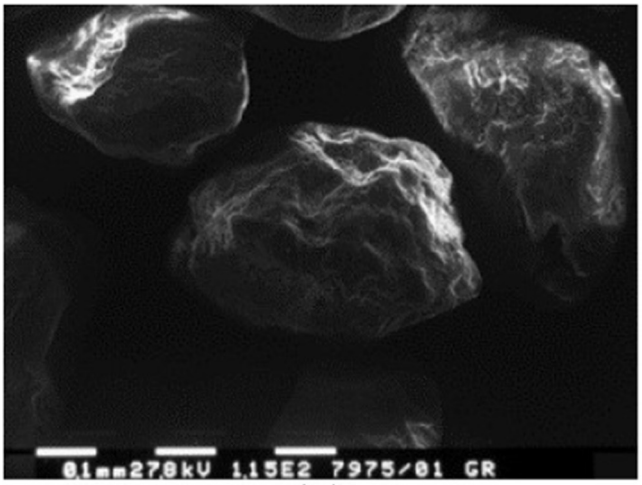

Fig. 2. SEM images of Fossanova S3 (a. from Iolli et al., 2015) and Hostun H31 sand (b. from Alikarami et al., 2015).

be positioned with a small amount of uncertainty being reached from both upper and lower sides (*i.e.*, contracting and dilating soils) (Fig. 3a). It is worth noting that the latter circumstance is strictly conditioned by the ability to control the density during the sample preparation. In fact, in the case of steel spheres (Fig. 3b), the possibility of forming very loose assemblies was hampered by the high self-weight and limited the friction resistance of the particles. In this second series of experiments, therefore, the CSL was always reached from the lower side. However, the uncertainty in the CSL positioning can be accepted considering that the deformation was reasonably homogeneous and the residual dilatancy at the end of the tests was limited (Modoni and Gazzellone, 2011).

This procedure, repeated for the extension tests, leads to a similar phenomenology (Fig. 4), but the most relevant outcome is that steadiness is reached at denser states when compared to compression. In fact, the two CSL traces, one interpolating the last points of the extension tests and the other copied from Fig. 3, reported here for reference, show a clear divergence with the increasing mean effective stresses.

A non-trivial aspect is that the same difference is noticed for both the natural soil and the steel sphere assembly. In the former case, a preferential orientation of the soil fabric, produced with deposition and persisting along with shearing, can be supposed (*e.g.*, Nakata et al. 1998; Yoshimine et al., 1998; Balakrishnaiyer et al., 1998; Flora et al., 2013), while anisotropy must be fully excluded in the latter case. In fact, even though the deposition in the gravitational field could generate the initial preferential orientation of the contacts, this effect is likely to be erased by the subsequent isotropic loading at large stresses (*e.g.*, Oda, 1972).

With regard to the CSL determination in the stress invariant plane, critical stress ratio M (Eq. (1)) has been obtained by extrapolating the results obtained at relatively small strains in order to limit the effects of the discontinuities. Critical stress ratio M has been estimated for each material as the intermediate value between those obtained at the peak and maximum contraction (Negussey et al., 1988; Flora and Modoni, 1998). As for the volumetric plane, the summary reported in Table 2 reveals that a

Table 1
Experimental program (ε_a axial strain; σ'_r radial effective stress) on Fossanova S3 sand (left) and steel spheres assemblies (right).

ID	Initial p′ (kPa)	Stress path	e_0	ID	Initial p′ (kPa)	Stress path	e_0
FCD50	50	$\varepsilon_a > 0$ – const σ'_r	0.510	SC50	50.40	$\varepsilon_a > 0$ – const σ'_r	0.649
FCL50			0.744	SEP100	110.20	$\varepsilon_a < 0$ – const p'	0.640
FCD100	100	$\varepsilon_a > 0$ – const σ'_r	0.512	SC200	201.67	$\varepsilon_a > 0$ – const σ'_r	0.624
FCL100			0.689	SE200	204.37	$\varepsilon_a < 0$ – const σ'_r	0.640
FED100		$\varepsilon_a > 0$ – const σ'_r	0.514	SC350	356.43	$\varepsilon_a > 0$ – const σ'_r	0.620
FEL100			0.730	SE350	366.53	$\varepsilon_a < 0$ – const σ'_r	0.630
FCD200	200	$\varepsilon_a > 0$ – const σ'_r	0.521	SCP400	409.73	$\varepsilon_a > 0$ – const p'	0.620
FCD400	400	$\varepsilon_a > 0$ – const σ'_r	0.522	SE400	362.07	$\varepsilon_a < 0$ const σ'_r	0.640
FCL400			0.695	SEP400	412.43	$\varepsilon_a < 0$ – const p′	0.626
FED400		$\varepsilon_a < 0$ – const σ'_r	0.528	SC500	499.03	$\varepsilon_a > 0$ – const σ'_r	0.630
FEL400			0.691	SE500	431.77	$\varepsilon_a < 0$ – const σ'_r	0.620
FCD700	700	$\varepsilon_a > 0$ – const σ'_r	0.547	SCP600	583.27	$\varepsilon_a > 0$ – const p′	0.610
FEL700		$\varepsilon_a < 0$ – const σ'_r	0.676	SE600	604.37	$\varepsilon_a < 0$ – const σ'_r	0.620

Please cite this article in press as: Salvatore, E. et al., Determination of the critical state of granular materials with triaxial tests, Soils Found. (2017), https://doi.org/10.1016/j.sandf.2017.08.005

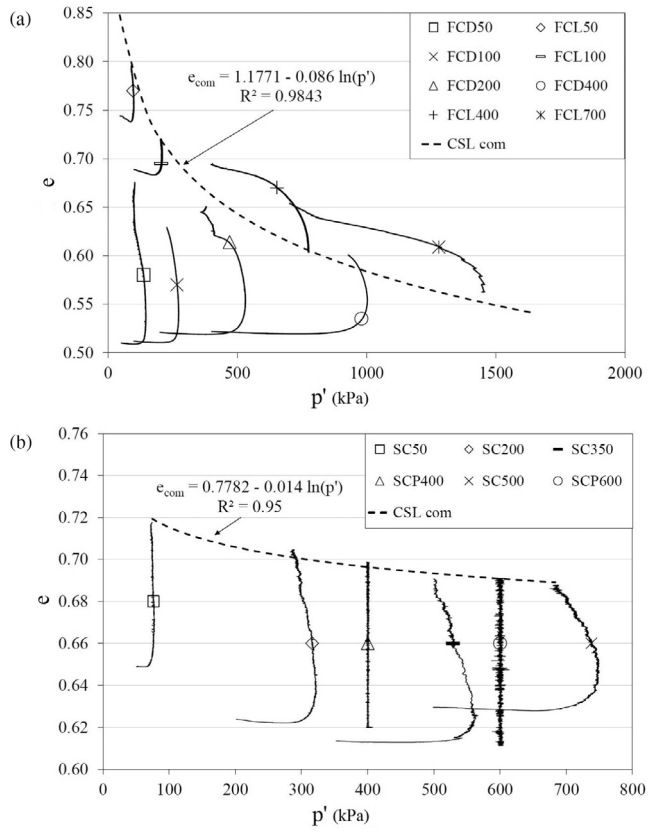

Fig. 3. Experimental determination of CSL trace in the *e-p'* plane for the Fossanova S3 sand (a) and for the steel spheres assembly (b).

unique value for M cannot be inferred for either compressional ($\sigma'_1 > \sigma'_2 = \sigma'_3$) or extensional ($\sigma'_1 = \sigma'_2 > \sigma'_3$) stress states. The comparison among the friction angles and the strength variables, defined by Lade and Duncan (1975) (Eq. (2)) and by Matsuoka and Nakai (1982) (Eq. (3)), shows that much lower differences are seen for the latter two cases.

$$LD_{com} = \frac{\sigma'_1 + 2\sigma'_3}{\sigma'_1 \cdot \sigma'^2_3} \tag{2.a}$$

$$LD_{ext} = \frac{2\sigma'_1 + \sigma'_3}{\sigma'^2_1 \cdot \sigma'_3} \tag{2.b}$$

$$MN_{com} = \frac{(\sigma'_1 + 2\sigma'_3) \cdot (\sigma'^2_3 + 2\sigma'_1\sigma'_3)}{\sigma'_1 \cdot \sigma'^2_3} \tag{3.a}$$

$$MN_{ext} = \frac{(2\sigma'_1 + \sigma'_3) \cdot (\sigma'^2_1 + 2\sigma'_1\sigma'_3)}{\sigma'^2_1 \cdot \sigma'_3} \tag{3.b}$$

3. Tests With X-ray tomography

In order to find an explanation for the above observation, the field of strain generated within a sample by compression and extension has been investigated with X-ray tomography. This technique involves the application of the 3D Digital Image Correlation method (DIC) to the three-dimensional images of the sample obtained step-by-step with an X-ray scanner while testing.

The adopted equipment (X-ray CT scanner housed in the Laboratoire 3SR of Grenoble) includes a triaxial testing device capable of simultaneously controlling the confining stress and axial strain on a sample with a diameter of 11 mm and a height of 22 mm (Fig. 5). Such small dimensions lead to an acceptable balance between the representativeness of the sample and the resolution of the resulting X-ray images.

However, in order to investigate the role of sample dimensions, compression and extension tests were repeated on the same material (Hostun sand) in the large apparatus used for the previous experimentation with a sample diameter and a height of 70 and 140 mm, respectively (Fig. 6). The samples in the two cases were prepared with the same methodology and yielded approximately the same dry density. The only difference between the two apparatuses was related to the end platens; in fact, the lower base was forced to translate without rotation in the larger apparatus and allowed to rotate freely in the smaller one. The stress relaxation periodically observed during the tests in the small apparatus is a direct consequence of stopping the loading system, necessary for performing the X-ray scan.

Apart from this secondary effect, the curves obtained in the smaller apparatus are more irregular and the contractive or dilative tendency of the soil subjected to the different loading conditions is enhanced. Such effects, also noticed by Huang et al. (2014), can be justified considering that the larger samples contain a higher number of particles; and thus, their behaviour is the homogenised summary of more portions, each of them deforming in a different manner.

The scanning of the small samples was alternated with loading in a stepwise sequence. The strain ramp, proceeding at a rate of 1% per hour, was, in fact, subdivided into several steps of 1–2% axial strain, after which a complete scanning process was performed. In order to obtain a three-dimensional reconstruction of the grain position, the sample, placed between the X-ray source and the detector, was continuously rotated around its vertical axis by 360°, while 1024 X-ray radiographs were acquired. The whole set of radiographs, representing the Radon's transform of the sample, forms the input of an inversion process (Natterer, 1986) that leads to the three-dimensional field of the X-rays' linear attenuation coefficient, practically proportional to the density of the investigated material. Starting from 2D images of 1250×1600 pixels, 3D images with a voxel size of 20×20×20 μm were reconstructed. Considering the fact that voxels are much smaller than soil particles (Fig. 1), it was possible to identify the position of each grain with sufficient accuracy.

The field of displacements produced between two subsequent loading steps is accomplished with 3D Digital Image Correlation software called TomoWarp2 (Andò et al., 2013), developed between Laboratoire 3SR and the

Please cite this article in press as: Salvatore, E. et al., Determination of the critical state of granular materials with triaxial tests, Soils Found. (2017), https://doi.org/10.1016/j.sandf.2017.08.005

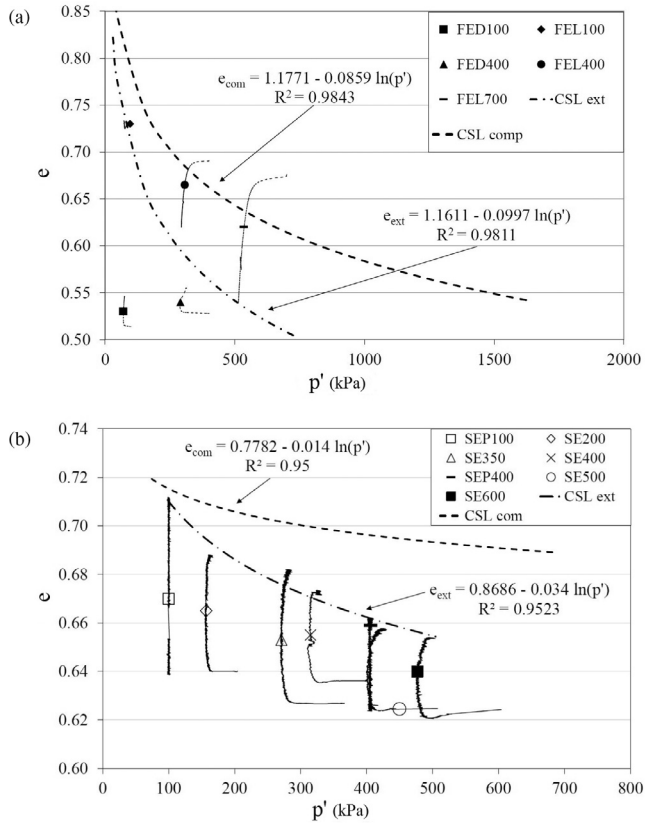

Fig. 4. Experimental determination of the CSL trace in the e-p′ plane for extension tests on Fossanova S3 sand (a) and steel spheres assemblies (b).

University of Lund. A grid of 1535 measurement nodes, each centred in a cubic cluster of 540 μm side (correlation window), is defined in the first 3D image of the sample. The displacement of each node, formed by three translational and three rotational components, is computed by tracking the corresponding cluster in the subsequent image by means of a best matching procedure. Deformation is then computed following the Green-Lagrange definition of the strain tensor in the large deformation framework (Holzapfel, 2002).

The full set of tests performed on Hostun H31 sand is reported in Table 3. A series of tests was firstly performed by Alikarami et al. (2015), who subjected samples of sand compacted at initial void ratios of 0.51–0.61 to triaxial compression tests ($\varepsilon_a > 0$) at various confining stresses (σ'_r ranging from 100 to 3000 kPa). The results obtained with the classical external measurement of displacements show the typical response of granular material, where dilatancy is suppressed by the increase in confining stress (Fig. 7). Similar effects were noticed in another series of extension tests ($\varepsilon_a < 0$) specifically performed on samples of the same soil formed at initial void ratios of 0.64–0.70 and subjected to monotonic loading (varying confining stresses σ'_r between 100 and 3000) (Fig. 8).

Since the adopted experimental tools enable the quantification of density and strains at the local scale, all tests were reanalysed by mapping the spatial distribution of these quantities. In particular, it was decided that focus would be placed on the patterns of distortional strain and soil porosity, following their changes throughout the tests. At various instants, the soil porosity was computed for each cluster of previously defined grid nodes looking at the 3D map of material density represented by greyscale images. After defining the thresholds to mark the transition from solid to empty spaces, the void ratio is computed as the ratio between the numbers of empty and full voxels within the cluster. The maps obtained at the end of the compression and extension tests, plotted in Fig. 9, show largely inhomogeneous spatial distributions, with the higher void ratios concentrated in the relatively narrow zones of the samples.

The most important observation concerns the role of the stress path, as very different patterns occur from compressive or extensive tests. In the compression tests, larger voids tend to form along the shear planes cutting the sample from side to side, while in the extension tests, the voids mainly concentrate within small restricted sections. In both cases, only limited portions of the sample are affected by large distortional and volumetric deformations, whereas the remaining parts remain almost frozen in their current states. Since this observation is systematic for all tests, there is an obvious dependency of the strain distribution on a number of concurrent factors, including loading direction, sample shape and boundary restraints. Similar effects were noticed by Lam and Tatsuoka (1988) who showed that slender samples are more prone to localized deformation during extension. In the present study, the different levels of rigidity of the upper and lower bases, in comparison to the softer lateral membrane, seem to dominate the deformation mechanism, turning into shear bands when $\sigma'_a > \sigma'_r$ (compression) and necking when $\sigma'_a < \sigma'_r$ (extension).

The above occurrence takes place more evidently in cases of gross strain localization, but can also be seen for apparently uniform samples. For instance, two cases are reported in Fig. 10, one for compression (Fig. 10a) and

Table 2
Critical strength parameters obtained from compression and extension tests.

		M	ϕ′ (°)	LD	MN
Fossanova sand S3	Compression	1.46	36.0	51.92	13.21
	Extension	1.05	39.6	49.38	14.44
Steel spheres	Compression	0.90	23.0	34.44	10.45
	Extension	0.74	25.0	34.29	10.73

Please cite this article in press as: Salvatore, E. et al., Determination of the critical state of granular materials with triaxial tests, Soils Found. (2017), https://doi.org/10.1016/j.sandf.2017.08.005

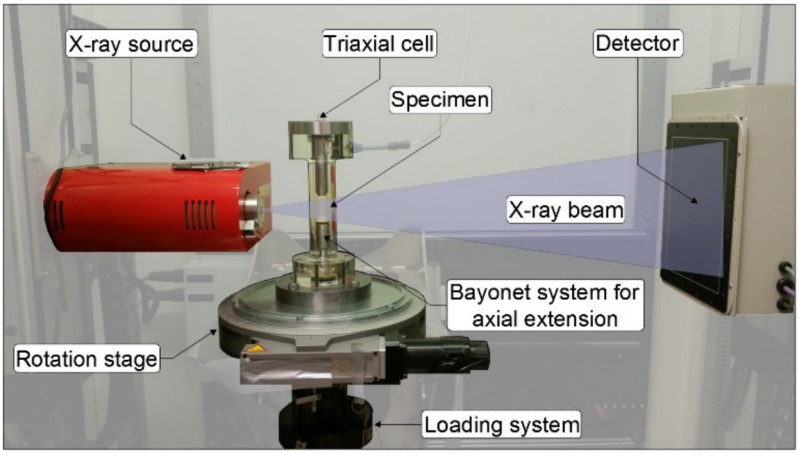

Fig. 5. Setup of the triaxial equipment in the X-ray scanner.

the other for extension (Fig. 10b), where the samples deformed in an apparently uniform way. Fig. 10a reports the spatial distribution of density on a sample of Hostun sand subjected to compression (Desrues, 2004) with the darker areas representing lower soil density. Although gross shear bands are missing, as these samples ended in the classical barrel shape, the dominating role of the two rigid frictional platens is quickly evident. The radial expansion activated by compression is in fact prevented in the upper and lower portions of the soil by the frictional tangential stresses developing at the two platens. Thus, two conical wedges are formed that protrude into the central portion of the sample pushing aside the soil and forming a pattern of radial cracks.

A different mechanism is shown in Fig. 10b reporting the field of shear strain in the last step of the HNEES02 extension tests. Strains are again localized into three portions of the sample, two near the end platens and the other in the middle portion, while the state of the rest of the sample does not change very much. The vertical and horizontal cross sections, taken at different depths, show again the presence of a conical wedge generated by the friction at the end platens. This time, the conical surface is subhorizontal, while the one observed in the compression tests is more inclined on the horizontal plane, similar to the shear bands depicted in Fig. 9.

In all cases, the localization occurs differently for the compression and extension tests, and this could explain the stress path dependency of the CSL trace in the e–p' plane. Indeed, the above results show that the uniformity of the sample deformation at the end of the tests is questionable and that any conclusion on the CSL, based on the assumption that the sample as a whole represents a soil element, is wrong.

Therefore, another possible option is to look at the sample as a model of the finite dimension and the triaxial test as a variation in the boundary conditions. From this viewpoint, the occurrence of the highest porosity in the zones, characterized by the largest distortion, suggests making a distinction among the different zones of the sample and assuming that the Critical State is attained only for a limited portion of the sample. Following this idea, the void ratio is selectively evaluated in the zones where major deformation takes place, looking at the patterns of distortional strain and at their statistical distribution in the final state of each test. The example in Fig. 11 shows the analysis performed in the last step (from 16% to 18% axial strain) of the HNEES02 extension test. In the left plot (Fig. 11a), the clusters where distortional strain exceeds the prescribed threshold (fixed equal to the mean plus one standard deviation of the distribution throughout the sample) are selected. Thereafter, the void ratio is computed by averaging the values measured in these zones only (Fig. 11b). It is worth noting that, even though the sample distortion seems to be apparently uniform until the end of the tests, the deformation is still localized within limited portions of the sample.

This analysis is then repeated for all tests, and the void ratios computed in the most deformed zones are reported (Fig. 12) as functions of the mean effective stress applied at the end of the tests (p_f'), distinguishing the data from the compression and extension tests with different symbols. In the same figure, the void ratios, obtained by averaging the local values all over the samples, are reported with full dots for comparison. These values are in fact similar to those cumulatively computed with the conventional measurement.

All curves show a significant reduction in the void ratio with the mean effective stress, in accordance with the observation previously obtained for larger samples (Figs. 3 and 4). Similarly, as before, there is a difference between the compression and extension tests, with the smaller ultimate void ratios occurring in the latter case. However, the most striking result is that such a difference disappears when the void ratios are computed locally in the most deforming zones. Although with larger scattering, possibly

Please cite this article in press as: Salvatore, E. et al., Determination of the critical state of granular materials with triaxial tests, Soils Found. (2017), https://doi.org/10.1016/j.sandf.2017.08.005

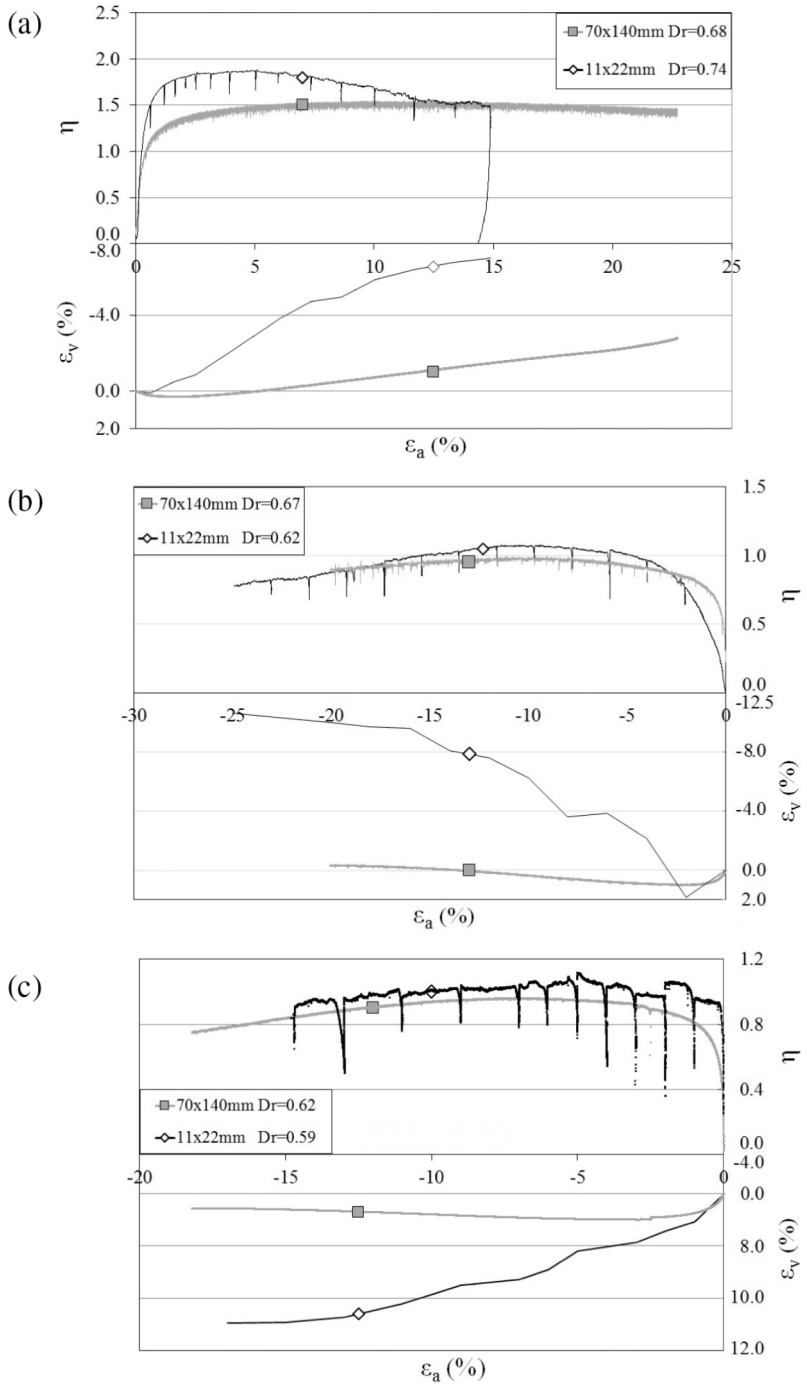

Fig. 6. Comparison between tests performed on the large (70×140 mm) and small (11×22 mm) samples of Hostun sands (a. compression at constant = 100 kPa confining stress; b. extension at constant = 100 kPa confining stress; c. extension at constant = 430 kPa confining stress).

due to the fact that the void ratio is computed in narrower zones, the data obtained from compression and extension do not show clearly distinguished alignments, as the open dots located on the same curve are located above the two lines obtained with the conventional measurement. Considering that all portions of the sample start from the same initial void ratio, there is an obvious tendency to dilation in the zones where larger distortion takes place, in comparison to the rest of the sample. This dilatant effect is superposed to the global contractive tendency of the soil (Figs. 7 and 8). Such a result can be considered as an effect of the different fabric evolution taking place at the local scale throughout the sample (Gao and Zhao, 2013).

4. Conclusions

The observation that the Critical State Locus (CSL) found for axisymmetric loading might depend on the

Please cite this article in press as: Salvatore, E. et al., Determination of the critical state of granular materials with triaxial tests, Soils Found. (2017), https://doi.org/10.1016/j.sandf.2017.08.005

Table 3
Experimental program performed on the Hostun H31 sand.

ID	Initial p′ (kPa)	Stress path	e_0
HNEA01	100	$\varepsilon_a > 0$ – const σ'_r	0.61
HHEA05	1000		0.53
HHEA04	2000		0.54
HHEA06	3000		0.52
HNEES02	100		0.68
HNEES01	430	$\varepsilon_a<0$ – const σ'_r	0.70
HHEES01	1000		0.68
HHEES02	3000		0.64

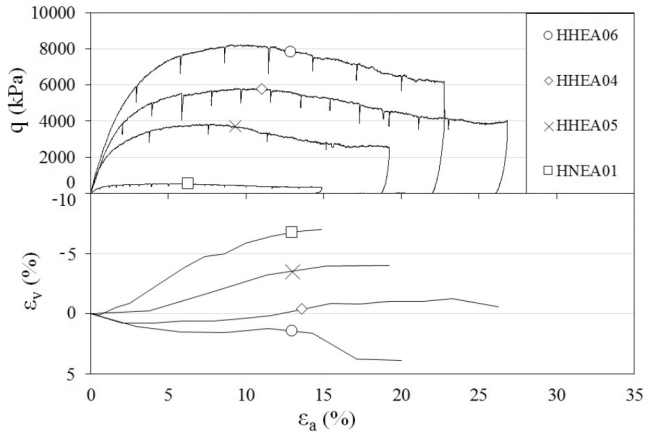

Fig. 7. Triaxial compression tests (modified from Alikarami et al., 2015).

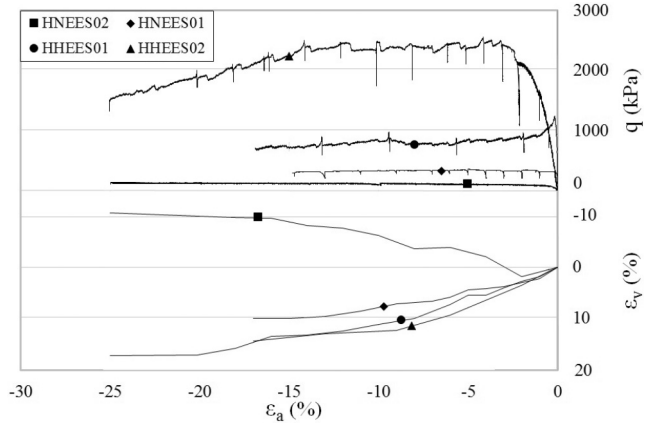

Fig. 8. Triaxial extension tests on samples of Hostun H31 sand.

induced strain path suggests reconsidering the role of triaxial tests in the current practice. Nowadays, Critical State models are calibrated with triaxial compression tests assuming samples as unit soil elements. CSL parameters are then applied to more general stress paths based on the principle that the initial soil fabric and a memory of the loading history are erased at the large deformations necessary to reach the Critical State. The uncertainty related to such a hypothesis poses serious concerns that often lead researchers to abandon the Critical State theory for the sake of more empirical models.

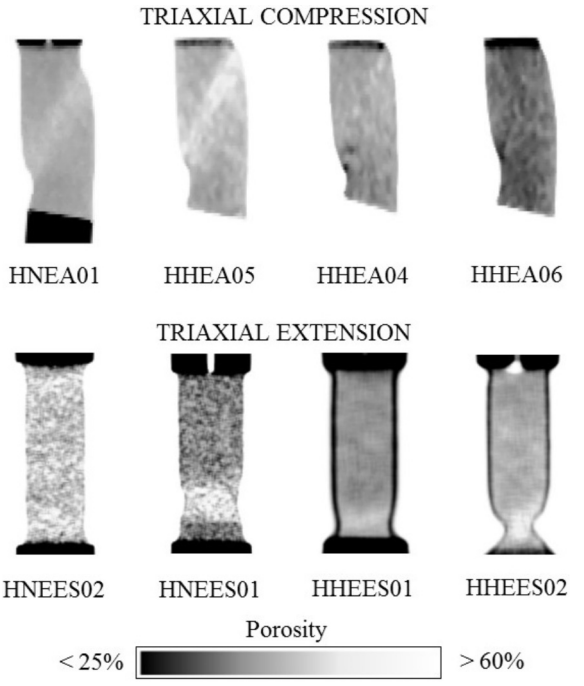

Fig. 9. Porosity maps at the end of compression and extension tests.

Willing to explore the validity of the above procedure, a comprehensive campaign has been undertaken, subjecting different granular materials to classical triaxial compression and extension tests and evaluating the soil state reached at the end of the tests. The results, based on the external measurement of the displacements (*i.e.*, providing a summary response of the sample), confirm that the soil heads to systematically different CSL in the *e-p′* plane when sheared under compression or extension, with a tendency to final denser states after extension. Such a result has noticeable implications on the overall predictive capability of the models, as the contractive or dilative tendency of the soil seen in triaxial compression tests (often related to state variable ψ introduced by Jefferies, 1993) might be wrong for the stress path other than compression. The occurrence of such a phenomenon, also for assemblies of steel spheres, implies that an explanation cannot be solely sought in the anisotropic shape of particles, as is done with tensors quantifying the initial fabric of the material and its evolution (Li and Dafalias, 2012), but also in the different deformation mechanisms taking place upon compression and extension. This conclusion might suggest generalizing the CSL concept, postulating a dependency of its constitutive parameters (Eq. (1)) on the loading direction.

In order to gain a deeper insight into the mechanisms activated within the sample, a second set of experiments has been carried out. A number of small sand samples has been subjected to triaxial extension tests and the results have been compared with those of compression tests on the same material (Alikarami et al., 2015). In both cases, punctual tomographic scans have been performed during the tests, processing images with the digital correlation

Please cite this article in press as: Salvatore, E. et al., Determination of the critical state of granular materials with triaxial tests, Soils Found. (2017), https://doi.org/10.1016/j.sandf.2017.08.005

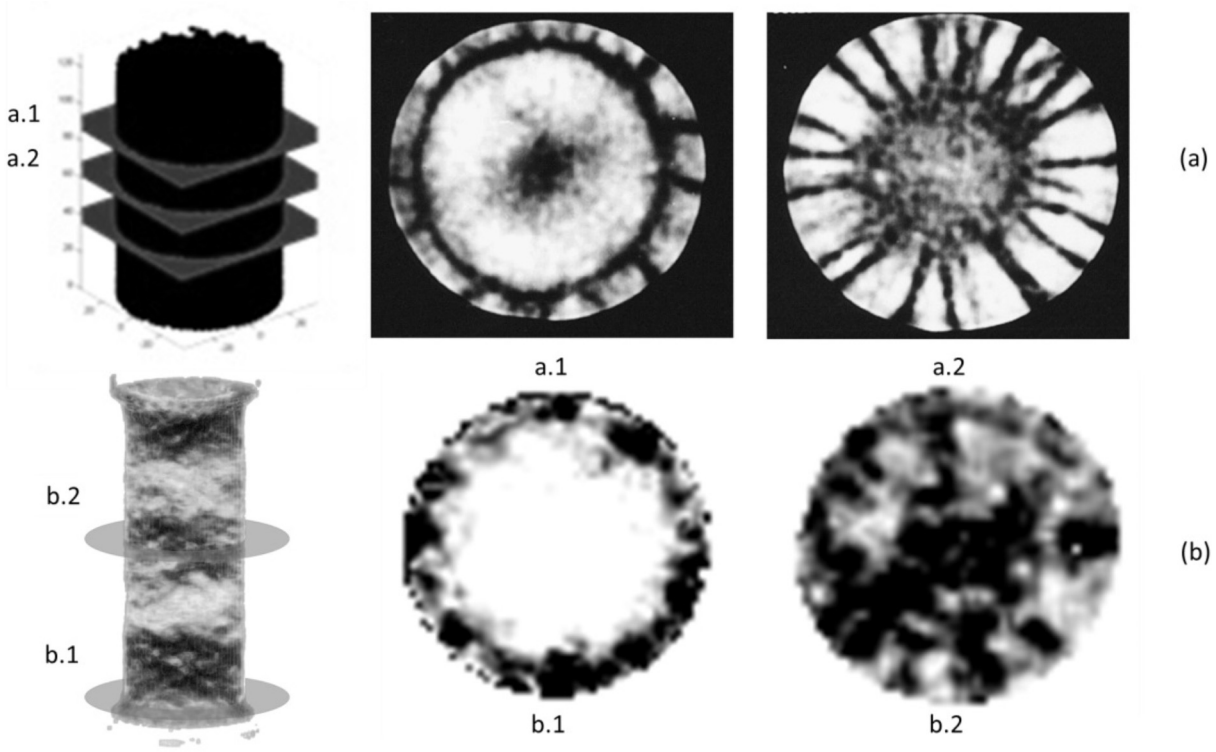

Fig. 10. Maps of density seen at the end of a compression tests by Desrues (2004) (a) and of distortional strains at the end of HNEES02 extension test (b).

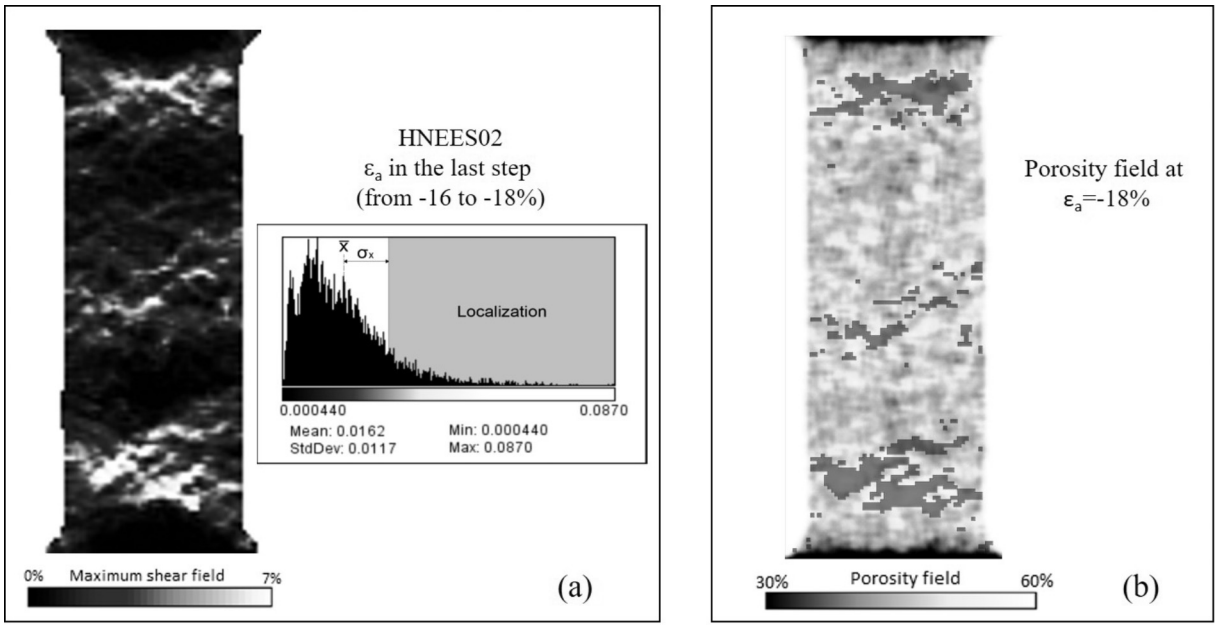

Fig. 11. Map and statistical distribution of the distortional strains (a) and void ratio (b) in the last step of the HNEES02 test (triaxial extension).

technique to derive the local distribution of the continuum variables from the positions and displacements of grains. All the tests showed a tendency for the deformation to concentrate within limited portions of the sample, also in the case where apparently uniform deformation is taking place (*i.e.*, barrel-shaped compressed samples or elongated samples not showing necking). This result, previously shown for compression tests by Desrues (2004) and here seen for extension tests (Fig. 10), seems to be the main reason for the observed influence of the loading directions on the CSL. In fact, while the state variables quantified by the global external measurements head to different final states for compressive or extensive loading, a unique final locus is seen in the most deforming zones (the portions supposed

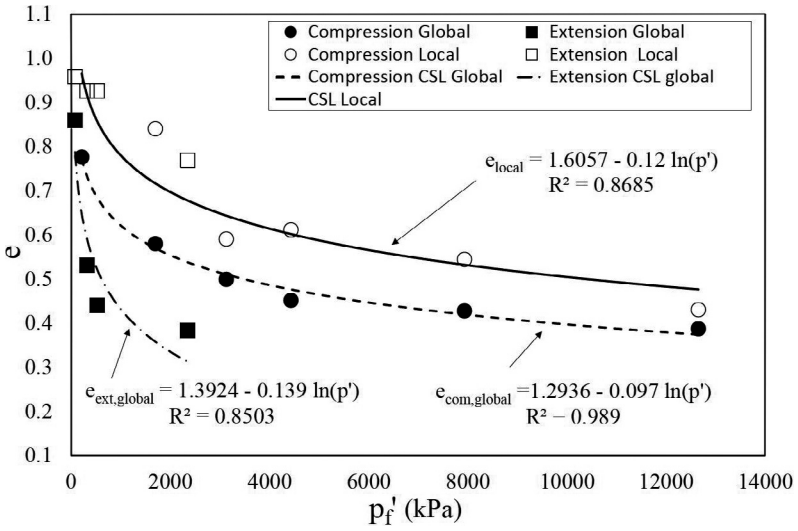

Fig. 12. Representation of the volumetric state at the end of compression and extension tests.

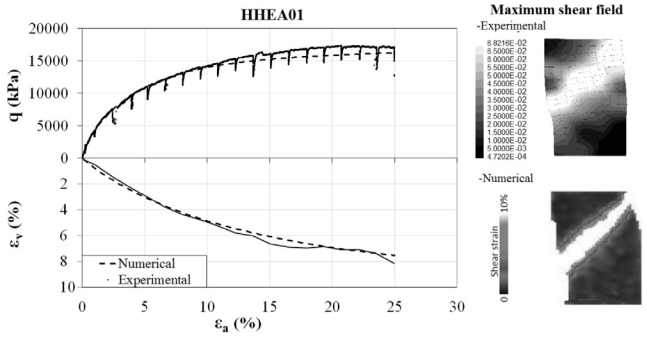

Fig. 13. Experiment vs numerical simulation of a compression test on Hostun H31 sand carried out at 7000 kPa constant confining stress.

to reach the critical state). Thus, the different CSL positions seen in the traditional tests seem to be due to the patterns of strain localization activated by compression and extension in combination with the different boundaries (flexible membrane and rigid end platens). Evidence of gross strain localization was already noticed by Lam and Tatsuoka (1988), but the validity of a unique CSL at the local scale can be postulated thanks to the present micromechanical investigation.

This result suggests reconsidering the extension of the CSL in a different way from simple shear to triaxial loading, together with the procedure adopted to calibrate the Critical State parameters. In fact, considering the uniqueness of the Critical State Locus at the local scale, its identification can be accomplished by solving a boundary value problem, *i.e.*, considering the triaxial sample as a small-scale model subjected to peculiar boundary conditions, different for compression or extension, and not as a homogeneously deforming unit element. Although more complex, the suggested calibration procedure would lead to obtaining a set of parameters for the CSL of general validity, *i.e.*, independent of the loading condition, and thus, extendable to any stress state.

An example of the suggested approach can be seen in Fig. 13, where compression tests on Hostun sand, carried out at a constant confining stress of 7000 kPa, have been reproduced with a finite difference code (ITASCA, 2005). In the simulation, a constitutive model (Dafalias et al., 2004) based on the Critical State, has been adopted assigning the Critical State parameters derived locally to the material (Fig. 12) and considering the spatial distribution of the initial void ratios seen with the tomographic measurement at the beginning of the tests. The figure shows not only the capability of the adopted constitutive model to capture the global stress strain response of the soil, but also that the spatial variability of the density within the sample may justify the asymmetric pattern of strain localization. It is worth noting that this result could not be obtained for samples having a homogeneous distribution of the void ratio. The predictive capability of the models could also benefit from more detailed investigations (*e.g.*, Andò et al., 2013) and soil models (Li and Dafalias, 2012) able to more precisely quantify the possible anisotropy connected with the particulate nature of granular materials.

References

Andò, E., Hall, S.A., Viggiani, G., Desrues, J., 2013. Experimental micromechanics of granular media studied by X-ray tomography: recent results and challenges. Geotech. Lett. 3, 142–146.

Alikarami, R., Andò, E., Gkiousas Kapnisis, M., Torabi, A., Viggiani, G., 2015. Strain localisation and grain breakage in sand under shearing at high mean stress: insights from in situ X-ray tomography. Acta Geotech. 10 (1), 15–30.

Balakrishnaiyer, K., Koseki, J., Modoni, G., AnhDan, L. Q., Tatsuoka, F., 1998, Deformation characteristics at small strain levels of dense gravel. In: Geotechnics of Hard Soils and Soft Rocks, eds. by Evangelista and Picarelli, Balkema, 1, 423–430.

Please cite this article in press as: Salvatore, E. et al., Determination of the critical state of granular materials with triaxial tests, Soils Found. (2017), https://doi.org/10.1016/j.sandf.2017.08.005

Been, K., Jefferies, M.G., Hachey, J., 1991. The Critical State of Sands. Géotechnique 41 (3), 365–381.

Casagrande, A., 1936. Characteristics of Cohesionless Soil Affecting the Stability of Slopes and Earth Fills. J. Boston Soc. Civ. Eng. 1925–1940, 257–276, reprinted in contribution to soil mechanics.

Chiaro, G., Koseki, J., De Silva, L.I.N., 2013. A density- and stress-dependent elasto-plastic model for sands subjected to monotonic torsional shear loading. SEAGS Geotech. Eng. J. 44 (2), 18–26.

Dafalias, Y.F., Manzari, M.T., 2004. A simple plasticity sand model accounting for fabric change effects. J. Eng. Mech. 130 (6), 622–634.

Dafalias, Y.F., Paradimitriou, A.G., Li, X.S., 2004. Sand plasticity model accounting for inherent fabric anisotropy. J. Eng. Mech. 130 (11), 1319–1333.

Desrues, J., 2004. Tracking strain localization in geomaterials using computerized tomography. In: The Proc. of the 1st Int. Workshop X-ray Tomography for Geomaterials, Kumamoto, Japan; Lisse, The Netherlands: Balkema, 2004. pp. 15–41.

Flora, A., Modoni, G., 1998, Complex testing and simple analysis on coarse grained materials. In: Viggiani, C. (Ed.), Proceedings of a workshop on prediction and performance in geotechnical engineering, Hevelius, Napoli. pp 151–216.

Flora, A., Lirer, S., Silvestri, F., 2012. Undrained cyclic resistance of undisturbed gravelly soils. Soil Dynam Earthquake Eng 43, 366–379.

Flora, A., Lirer, S., 2013. Small strain shear modulus of undisturbed gravelly soils during undrained cyclic triaxial tests. Geotech. Geol. Eng. 31 (4), 1107–1122.

Fonseca, J., O'Sullivan, C., Coop, M.R., Lee, P.D., 2013. Quantifying the evolution of soil fabric during shearing using directional parameters. Géotechnique 63 (6), 487–499.

Gao, Z., Zhao J., 2013. Strain localization and fabric evolution in sand. Int. J. Solid Struct., 50, Elsevier Pub., pp. 3634–3648.

Gajo, A., Muir Wood, D., 1999. A kinematic hardening constitutive model for sands: the multiaxial formulation. Int. J. Numer. Anal. Meth. Geomech. 23, 925–965.

Holzapfel, G.A., 2002, Nonlinear Solid Mechanics: A Continuum Approach for Engineering Science. In: Meccanica 37 (4), 489–490, Kluwer Academic Publisher.

Huang, X., Hanley, K.J., O'Sullivan, C., Kwok, F.C.Y., 2014. Effect of sample size on the response of DEM samples with a realistic grading. Particuology 15, 107–115.

Iolli, S., Modoni, G., Chiaro, G., Salvatore, E., 2015. Predictive correlations for the compaction of clean sands. Transport. Geotech. 4, 38–49.

Itasca, 2005. Fast Lagrangian Analysis of Continua. Itasca Consulting Group, Minneapolis, USA.

Jafarian, Y., Ghorbani, A., Salamatpoor, S., Salamatpoor, S., 2013. Monotonic triaxial experiments to evaluate steady-state and liquefaction susceptibility of Babolsar sand. J. Zhejiang Univ., Sci. A (Appl. Phys. Eng.) 14 (10), 739–750.

Jefferies, M.G., 1993. Nor-sand: a simple critical state model of sand. Geotechnique 43 (1), 91–103.

Lade, P.L., Duncan, J.M., 1975. Elastoplastic stress-strain theory for cohesionless soil. J. Soil Mech. Found.. Div. ASCE 101, 1037–1053.

Lam, W.K., Tatsuoka F., 1988, Triaxial compressive and extension strength of sand affected by strength anisotropy and sample slenderness, Advanced Triaxial Testing of Soil and Rock, ASTM STP 977, Donaghe, Chaney and Marshall Silver Eds. American Society of Testing Materials, Philadelphia, 1988. pp. 655–666.

Li, X.S., Dafalias, Y.F., 2002. Constitutive modelling of inherently anisotropic sand behaviour. J. Geotech. Geoenviron. Eng. ASCE 128 (10), 868–880.

Li, X.S., Dafalias, Y.F., 2012. Anisotrpic Critical State Theory: role of fabric. J. Eng. Mech., ASCE 138 (3), 263–275.

Manzari, M.T., Dafalias, Y.F., 1997. A critical state two surface plasticity model for sands. Géotechnique 47 (2), 255–272.

Matsuoka, H., Nakai, T., 1982, A new failure criterion for soils in three dimensional stresses, IUTAM Conference on Deformation and Failure of Granular Materials. Delft, pp. 253–263.

Modoni, G., Koseki, J., Anh Dan, L.Q., 2011. Cyclic stress strain response of compacted gravel. Géotechnique 61 (6), 473–485.

Modoni, G., Gazzellone, A., 2011, Experimental Observations on the Critical State of Granular Materials. In: Kim, Ki et al. (Eds.), International Symposium on Deformation Characteristics of Geomaterials, September 1–3, 2011, Seoul (Korea), IOS Press, pp. 850–857.

Mooney, M.A., Finno, R.J., Viggiani, M.G., 1998. A Unique Critical State for Sand? In: J. Soil Mech. Fdns. Div., ASCE 124(11), 1100–1108.

Muir Wood, D., Belkheir, K., Liu, D.F., 1994. Strain softening and state parameter for sand modelling. Geotechnique 44 (2), 335–339.

Nakata, Y., Hyodo, M., Murata, H., Yasufuku, N., 1998. Flow deformation of sands subjected to principal stress rotation. Soils Found. 38 (2), 115–128.

Natterer, F., 1986. The Mathematics of Computerized Tomography, Classics in Applied Mathematics, 32, Soc. Indust. Appl. Math., John Wiley and Sons, 221 pp.

Negussey, D., Wijewickreme, W.K.D., Vaid, Y.P., 1988. Constant volume friction angle of granular materials. Can. Geotech. J. 25 (10), 50–55.

Oda, M., 1972. Initial fabrics and their relations to mechanical properties of granular materials. Soils Found. 12 (1), 17–36.

Oda, M., Nakayama, H., 1988. Introduction of inherent anisotropy of soils in function. In: Satake, M., Jenkins, J.T. (Eds.), Micromechanics of Granular Materials. Science Pub, Amsterdam, pp. 81–90.

Papadimitriou, A.G., Dafalias, Y.F., Yoshimine, M., 2005. Plasticity modeling of the effect of sample preparation method on sand response. Soils Found. 45 (2), 109–124.

Poorooshasb, H.B., 1961, The Properties of Soils and Other Granular Media in Simple Shear, Ph.D. Thesis, Cambridge University.

Poulos, S.J., Castro, G., France, W., 1985. Liquefaction evaluation procedure. J. Geotechn. Eng. Divis., ASCE 111 (6), 772–792.

Reza Imam, S.M., Morgenstern, N.R., Robertson, P.K., Chan, D.H., 2005. A critical-state constitutive model for liquefiable sand. Can. Geotech. J. 42, 830–855.

Riemer, M.F., Seed, R.B., 1997. Factors affecting apparent position of steady-state line. J. Geotech. Geoenviron. Eng. (ASCE) 123 (3), 281–288.

Roscoe, K.H., Scholfield, A.N., Wroth, C.P., 1958. On the Yielding of soils. Geotechnique 8 (1), 22–53.

Scholfield, A.N., Wroth, P., 1968, Critical State Soil Mechanics, McGraw-Hill Book Co., London, p. 310.

Thurairajah, A., 1961. Some Shear Properties of Kaolin and of Sand. Ph. D. Thesis, Cambridge University.

Vaid, Y.P., Chern, J.C., 1985. Cyclic and monotonic undrained response of saturated sands. Advances in the Art of Testing Soils Under Cyclic Loading. ASCE, New York, pp. 120–147.

Vaid, Y.P., Chung, E.K.F., Kuerbis, R.H., 1990. Stress path and steady state. Can. Geotech. J. 27 (1), 1–7.

Vaid, Y.P., Thomas, J., 1995. Liquefaction and post liquefaction behaviour of sand. J. Geotech. Geoenviron. Eng. 121 (2), 163–173.

Verdugo, R., Ishihara, K., 1996. The steady state of sandy soils. Soils Found. 36 (2), 81–91.

Vesic, A.S., Clough, G.W., 1968. Behaviour of granular materials under high stresses. In: Proc. ASCE, J. Soil Mech. Found. Div., 94 (SM3), 661–688.

Wroth, C.P., 1958. Soil behaviour during shear – existence of critical void ratios. Engineering 186, 409–413.

Yoshimine, M., Ishihara, K., Vargas, W., 1998. Effects of principal stress direction and intermediate principal stress on undrained shear behavior of sand. Soils Found. 38 (3), 179–188.

Yoshimine, M., Kataoka, M., 2007, Steady state of sand in triaxial extension test. In: Proc. of the Int. Workshop on Earthquake Hazard and Mitigation, Guwahati, India, 7–8 December 2007.

Please cite this article in press as: Salvatore, E. et al., Determination of the critical state of granular materials with triaxial tests, Soils Found. (2017), https://doi.org/10.1016/j.sandf.2017.08.005